Stem Cells Translational Medicine, 2025, **14**, szaf044
https://doi.org/10.1093/stcltm/szaf044
Original Research

Microencapsulated 3D culture of human umbilical cord-derived mesenchymal stem cells enhances their therapeutic effect on intrauterine adhesion

Hongjiang Liu[1,2,3,‡], Xiaohua Jiang[2,3,4,‡], Jin Qian[2,3,4,‡], Xuan Xu[2,3,4], Shujun Yu[2,3,4], Zhongqin Tang[2,3,4], Ying Wang[2,3,4], Qiong Xing[2,3,4], Heng Tang[*,5], Jianye Wang[2,3,4,*], Zhaolian Wei[2,3,4,*]

[1]Department of Gynecology, Xuzhou Maternity and Child Health Care Hospital, Xuzhou, Jiangsu 221700, China,
[2]NHC Key Laboratory of Study on Abnormal Gametes and Reproductive Tract (Anhui Medical University), Hefei, Anhui 230032, China,
[3]Anhui Province Key Laboratory of Reproductive Health and Genetics, Hefei, Anhui 230032, China,
[4]Department of Obstetrics and Gynecology, the First Affiliated Hospital of Anhui Medical University, Hefei, Anhui 230022, China,
[5]Wanbei Coal Electric Group General Hospital, Anhui Province, Suzhou 234011, China

[*]Corresponding authors. Zhaolian Wei, Department of Obstetrics and Gynecology, the First Affiliated Hospital of Anhui Medical University, No 218 Jixi Road, Hefei 230022, Anhui, China. E-mail: weizhaolian@ahmu.edu.cn; Jianye Wang, Department of Obstetrics and Gynecology, the First Affiliated Hospital of Anhui Medical University, No 218 Jixi Road, Hefei 230022, Anhui, China. E-mail: wangjianye9@126.com; Heng Tang, Wanbei Coal Electric Group General Hospital, Anhui Province, Suzhou 234011, China. E-mail: tangheng@mail.ustc.edu.cn
[‡]H. Liu, X. Jiang, and J. Qian contributed equally to this work.

Abstract

Therapeutic application of mesenchymal stem cells is emerging as a potential strategy for the management of intrauterine adhesion (IUA). However, conventional 2D cultures often face issues such as insufficient cell quantities and suboptimal efficacy. In this study, we investigated the potential of microencapsulated 3D culture in enhancing the proliferation and stemness of human umbilical cord-derived mesenchymal stem cells (hUCMSCs), and their potential augmentation for antifibrotic treatment of IUA via the transforming growth factor beta 1 (TGF-β1)/Smad3 signaling pathway. Here, hUCMSCs were encapsulated in sodium alginate shells, and the microencapsulated 3D culture of hUCMSCs (3D-hUCMSCs) was harvested after removal of the encapsulation. We assessed the amount, cell proliferation, and the stemness gene expression of 3D-hUCMSCs and 2D cultured hUCMSCs. Subsequently, the therapeutic effect of 3D-hUCMSCs was evaluated by specific staining and mating experiments in the IUA mouse model. The expression of the TGF-β1/Smad3 signaling pathway was analyzed by western blot and quantitative real-time polymerase chain reaction. Our results showed that microencapsulated 3D culture significantly enhanced cell proliferation and elevated stemness gene expression, compared to traditional 2D culture. Furthermore, the endometrial thickness and number of glands increased, and the endometrial fibrosis and inflammation ameliorated in 3D-hUCMSCs administration. Moreover, 3D-hUCMSCs significantly inhibited the expression of the TGF-β1/Smad3 signaling pathway and restored the fertility. These findings indicate that microencapsulated 3D culture enhances cell proliferation and stemness of hUCMSCs. The 3D-hUCMSCs improved the endometrial recovery in structure and function. Microencapsulated 3D culture promoted the antifibrotic and anti-inflammatory effects of hUCMSCs in the treatment of IUA. This study introduces a novel strategy of microencapsulated 3D-hUCMSCs for IUA treatment.

Key words: umbilical cord-derived mesenchymal stem cells; microencapsulate; 3D culture; Intrauterine adhesions; TGF-β1/Smad3 signaling pathway.

Received: 21 December 2024; **Accepted:** 1 September 2025.

Graphical abstract

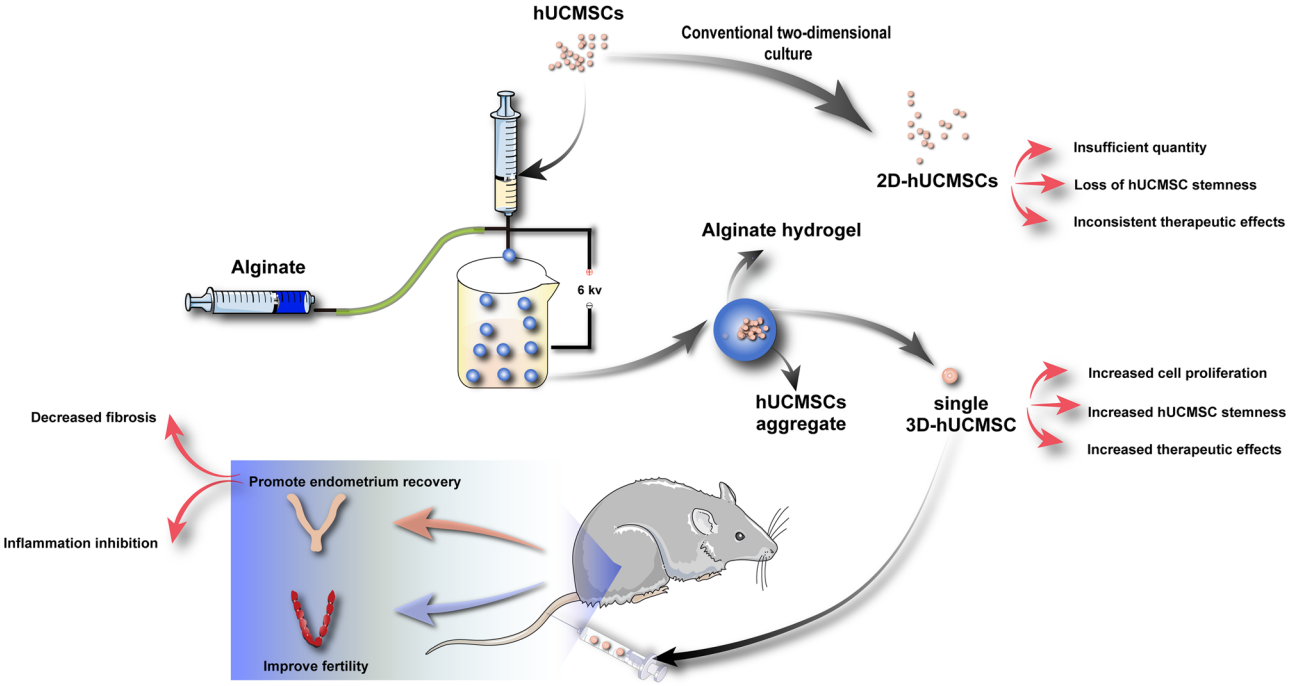

Significance statement

3D culture can enhance the stemness and therapeutic potential of mesenchymal stem cells (MSCs); however, the current commonly used 3D culture methods are not suitable for long-term culture and large-scale production of MSCs. In this study, we introduced a novel 3D culture method: microencapsulated 3D culture. We found that microencapsulated 3D culture enhances the proliferation and stemness of human umbilical cord-derived mesenchymal stem cells (hUCMSCs). The hUCMSCs after microencapsulated 3D culture improved the endometrial recovery in structure and function, and their antifibrotic effects were amplified in the treatment of IUA. These finding introduces a novel strategy of microencapsulated 3D hUCMSCs for IUA treatment.

Introduction

Intrauterine adhesion (IUA), also known as Asherman syndrome, typically occurs as a fibrotic repair response following injury to the basal layer of the endometrium, leading to partial or complete adhesion in the uterine cavity.[1] Conventional clinical treatments involve hysteroscopic adhesion release, hormonal therapy, and physical barrier therapy.[2,3] However, these approaches rely on the limited regenerative capacity of the endometrium and often result in recurrence.[4] Therefore, there is an urgent need of the innovative therapeutic approaches for IUA.

Intrauterine adhesion is characterized by severe endometrial damage or infection, cell proliferation and differentiation disorders, fibrous tissue replacement, and adhesion formation.[5] Inflammation is an important trigger of fibrosis, and persistent inflammation leads to local tissue fibrosis and loss of normal.[6] In fibrotic diseases, transforming growth factor beta 1 (TGF-β1) can promote the aggregation of fibroblasts and inflammatory cells, increase collagen synthesis and pro-inflammatory factor secretion, induce the synthesis of the extracellular matrix, and further promote tissue fibrosis.[7] Many evidences suggest that the TGF1/Smad pathway is associated with fibrosis. Li et al. reported that bone marrow stem cells combined with dihydroartemisinin can reverse renal fibrosis via targeting the TGF-β1/Smad pathway.

Mesenchymal stem cells (MSCs) are adult stem cells with self-renewal and multi-differentiation potential.[8] In recent years, MSCs have been widely applied in the regenerative medicine, including their potential use in treating IUA.[9,10] Umbilical cord-derived MSCs (UCMSCs) derived from postnatal umbilical cord tissue offer an ethically acceptable and more accessible source of stem cells. Umbilical cord-derived MSCs exhibit lower immunogenicity, stronger proliferation, and longer retention time after transplantation, making them a more promising therapeutic cell type.[11] Many researches and clinical trials found that UCMSCs increased endometrial thickness and alleviated IUA in patients within a short time.[12–14]

While MSCs present a potential clinical treatment for IUA, their clinical application still meets considerable challenges. Clinical treatments require a large quantity of high-quality MSCs, but conventional two-dimensional (2D) culture often fails to meet the clinical need, due to their low yield, suboptimal survival rate, and inconsistent therapeutic effects.[7,15,16] Furthermore, the 2D culture also leads to a loss of MSC stemness, thereby diminishing their therapeutic potential.[17] Three-dimensional (3D) culture of MSCs has emerged as an area of increasing interest. This technique allows for the cultivation of multicellular spheres using low attachment plate culture, thereby more accurately mimicking the in vivo environment.[18]

However, these prevalent spheroid culture methods, such as 3D microtiter and hanging drop, are inadequate for long-term culture.[19,20] To address these limitations, several studies have explored supportive materials for 3D growth and sustained retention of MSCs.[21–23]. For instance, the chitosan hydrogel/3D-printed poly (ε-caprolactone) was developed to incorporate MSCs, effectively enhancing the repair of articular cartilage injuries.[24] Despite these advancements, the mass production of MSCs with these scaffold materials remains challenging, and the efficacy of the resultant MSCs is still limited.

In this study, we introduced a 3D spheroid culture method, termed the cell microencapsulated culture technique, which encapsulates human UCMSCs (hUCMSCs) within a sodium alginate shell to construct microphysiological cell culture systems that mimics the *in vivo* microenvironment. This microencapsulated 3D culture is simple to implement, cost-effective, and easy for mass production. We investigated the effects of microencapsulated 3D culture on the characteristics of hUCMSCs, evaluated whether microencapsulated 3D culture of hUCMSCs could enhance the therapeutic efficacy in IUA mice, and explored the antifibrotic mechanism.

Materials and methods

Culture and characterization of hUCMSCs

Human umbilical cord-derived mesenchymal stem cells were obtained accroding to the method described in a previous study.[25] hUCMSCs were cultured in a 37 °C, 5% CO^2 conditioned incubator using Dulbecco's Modified Eagle Medium/Ham's F-12 (Gibco). The culture medium was supplemented with 10% fetal bovine serum (Gibco), 100 U/mL penicillin, and 100 mg/mL streptomycin (Biosharp, China). Upon reaching 80%-90% confluence, hUCMSCs underwent trypsin treatment for passaging. Cells at passages 4-6 were utilized in the experiments. To identify the hUCMSCs, flow cytometry was employed to detect the expression of surface markers, including positive CD44 and CD90, and negative CD34.

Microencapsulated 3D culture of hUCMSCs

Microencapsulated 3D culture of MSCs was generated by the coaxial electrospray system as in a previous study.[26] These cells were then mixed with 2 mg/mL rat tail tendon collagen I to serve as the core of the microcapsules. The microcapsule core and 20 mg/mL sodium alginate solution (purity 90%) were respectively injected into the inner and outer cavities of the coaxial channel. The coaxial channel liquids formed microdroplets under a high-voltage electric field and dropped into the calcium chloride solution, which rapidly gelatinized to form microcapsules. The flow rate ratio between the inner and outer cavities of the coaxial channel was 1:3.75. Microencapsulated 3D-hUCMSCs were cultured in the Modified Eagle Medium/Ham's F-12 with fetal bovine serum.

Cell proliferation and apoptosis

The sodium alginate shell was removed on day 5, and the hUCMSCs were collected after being digested by trypsin, referred to as 3D-hUCMSCs. The same procedure was applied to plate-cultured hUCMSCs, referred to as 2D-hUCMSCs. The obtained hUCMSCs were counted by a cell counter and diluted to the same cell concentration for the following experiments. (1) Cell Counting Kit-8 (CCK-8) assay: CCK-8 reagent (Solarbio) was added to the culture solution, and hUCMSCs were cultivated in 96-well plates for 2 h. The absorbance of each well was measured at 450 nm using a microplate reader (SpectraMAX iD3). (2) Apoptosis detection: hUCMSCs were incubated with Annexin V-FITC and Propidium Iodide (PI) (Beyotime) on ice for 20 minutes in the dark after resuspension in 200 μL of binding buffer. Apoptosis was analyzed by flow cytometry. (3) Cellular differentiation: cellular differentiation was confirmed by the Adipogenesis, Chondrogenesis, and Osteogenesis Differentiation Kits (Gibco) in accordance with the manufacturer's instructions.

Experimental animals and ethical approval

Female C57BL/6J mice aged 6-8 weeks were chosen for the experiment and housed in an Specific Pathogen Free lab (21-25 °C, humidity 40%-60%, 12-h light/12-h dark cycle) with unlimited access to sterilized food and water. These mice were procured from the Animal Center of Anhui Medical University. Ethical approval for all animal experimental protocols was obtained from the Animal Ethics Committee of Anhui Medical University.

Establishment of the IUA model

The IUA model was established following a previous study.[27] Mice were randomly divided into 4 groups: sham group, model group, Model + 2D-hUCMSCs treatment group (2D-hUCMSCs group), and Model + 3D-hUCMSCs treatment group (3D-hUCMSCs group), each containing 12 mice. After

Table 1. Primer sequence of genes used in qRT-PCR analysis.

Gene name	Forward primer sequence (5′-3′)	Reward primer sequence (5′-3′)
GAPDH-human	GGAGTCCACTGGCGTCTTCA	GTCATGAGTCCTTCCACGATACC
OCT4-human	GTGGTCCGAGTGTGGTTCTGTAAC	CCCAGCAGCCTCAAAATCCTCTC
SOX2-human	CAGCATGTCCTACTCGCAGCAG	CTGGAGTGGGAGGAAGAGGTAACC
KLF4-human	GGGACGGCTGTGGATGGAAATTC	CTTCATGTGTAAGGCGAGGTGGTC
c-MYC-human	AGCAGCGACTCTGAGGAGGAAC	TCCAGCAGAAGGTGATCCAGACTC
β-actin-mouse	CTACCTCATGAAGATCCTGACC	CACAGCTTCTCTTTGATGTCAC
TGF-β1-mouse	CCAGATCCTGTCCAAACTAAGG	CTCTTTAGCATAGTAGTCCGCT
Smad3-mouse	ATTCCATTCCCGAGAACACTAA	TAGGTCCAAGTTATTGTGTGCT
TNF-α-mouse	ATGTCTCAGCCTCTTCTCATTC	GCTTGTCACTCGAATTTTGAGA
IL-1-mouse	AATCTCGCAGCAGCACATCAAC	AGGTCCACGGGAAAGACACAG

Abbreviations: c-MYC, cellular-myelocytomatosis viral oncogene; GAPDH, glyceraldehyde-3-phosphate dehydrogenase; IL-1, interleukin-1; KLF4, Kruppel-like factor-4; OCT4, octamer-binding transcription factor-4; Smad3, SMAD family member 3; SOX2, SRY-related high-mobility-group-box protein-2; TGF-β1, transforming growth factor beta I; TNF-α, tumor necrosis factor alpha.

intraperitoneal injection of 1.25% tribromoethanol (AbMole) (0.4 mL/20 g weight), the mice were anesthetized, fixed in the supine position, and subjected to a 2.5 cm incision in the sterilized inferior abdomen. Uterus horns were exposed, injected with 95% ethanol for 20 seconds, and washed with phosphate-buffered saline solution thrice. Afterward, the uterus was returned, and abdominal wounds were closed. MSCs were encapsulated into 3D microcapsules on the modeling day. The sodium alginate shell was removed by sodium citrate on day 5, and the obtained MSCs were trypsinized into single-cell suspensions at a concentration of 1×10^6/mL, and injected via the tail vein to treat mice in the 3D-hUCMSCs group at 0.2 mL per mouse according to a previous study.[28] Mice in the 2D-hUCMSCs group were treated using equal cell numbers of 2D-hUCMSCs, while the model group was treated with equal volumes of saline. Seven days post-treatment, 24 mice ($n = 6$ per group) were sacrificed with uterine tissues and blood collected for subsequent experiments, while the remaining 24 mice ($n = 6$ per group) were utilized for mating experiments.

Hematoxylin and eosin staining

The mouse uterus was fixed in 4% paraformaldehyde (Beyotime), paraffin-embedded after dehydration, and sliced into 4 μm sections. Hematoxylin and eosin staining (Solarbio) was performed following routine procedures after deparaffinization and rehydration. Slide scanning using Pannoramic MIDI FL (3DHISTECH) enabled observation of the entire uterus image and counting of gland numbers. The average endometrial thickness was calculated from at least 5 randomly selected fields of view on each slide using ImageJ software (Image J 1.53e, National Institutes of Health).

Masson staining

Deparaffinized slices underwent sequential staining with Weigert's iron hematoxylin solution, lixin magenta solution, and aniline blue solution following the instructions of the Masson staining kit (Sbjbio). Differentiation and washing steps were performed accordingly. The ImageJ software was utilized to calculate the ratio of the collagen fiber area stained in blue to the total view.

Immunohistochemistry

After deparaffinization, dehydration, and antigen retrieval, slides were treated with hydrogen peroxide to block endogenous peroxidase activity per the manufacturer's instructions (ZGSB-BIO). The sections were then incubated overnight at 4 °C with primary antibodies against collagen I (Abcam, 1:1000, UK) and α-smooth muscle actin (α-SMA, Abcam, 1:1000, UK). Subsequent incubation with reaction enhancement solution and secondary antibody, followed by staining with 3,3′-diaminobenzidine (ZGSB-BIO) at room temperature, was carried out. The ImageJ software was employed to calculate the ratio of the positive area with brown staining to the total view.

ELISA assay

Mice were anesthetized to collect blood through a cardiac puncture. After centrifugation at 1000 g for 10 minutes at 4 °C, serum was collected and stored at −20 °C. Tumor necrosis factor alpha (TNF-α) and interleukin-1 (IL-1) were detected using their corresponding ELISA kits (MUTI SCIENCES, China).

Mating experiments

Seven days after treatment, female mice were mated with male C57/BL6J mice (10 weeks old) with confirmed fertility. The detection of the vaginal plug in the morning was considered day 0.5 of gestation. Female mice were sacrificed on day 10.5 of gestation to examine uterine pregnancy.

Quantitative real-time polymerase chain reaction

Total RNA was extracted using Trizol reagent (Thermo Fisher). RNA concentration and purity were assessed using a Ultraviolet-Visible spectrophotometer (Nanodrop 2000). Reverse transcription to complementary DNA was performed following the kit instructions (Biosharp). The primer sequences for relevant genes are provided in Table 1. Quantitative real-time polymerase chain reaction (qRT-PCR) was carried out using a PCR thermal cycler (Roche LightCycler480), and the expression levels of target genes were normalized to the housekeeping genes β-actin and glyceraldehyde-3-phosphate dehydrogenase (GAPDH) mRNA using the $2^{-}\triangle\triangle^{CT}$ method.

Western blot

Cell and tissue proteins were extracted using radioimmunoprecipitation lysis buffer (Beyotime), and concentrations were determined using a BCA Protein Assay kit (Beyotime). After densification in 5× sodium dodecyl sulfate-polyacrylamide gel electrophoresis loading buffer (Beyotime), proteins were separated in 10% polyacrylamide gels and transferred to polyvinylidene fluoride (PVDF) membranes (Millipore). PVDF membranes were incubated overnight at 4 °C with primary antibodies against octamer-binding transcription factor-4 (OCT4) (CST, 1:2000, US), SRY-related high-mobility-group-box protein-2 (SOX2) (CST, 1:2000, US), Kruppel-like factor-4 (KLF4) (Abcam, 1:2000, UK), cellular-myelocytomatosis viral oncogene (c-MYC) (Abcam, 1:2000, UK), TGF-β1 (Abcam, 1:2000, UK), Smad3 (Abcam, 1:2000, UK), and pSmad3 (Abcam, 1:2000, UK) after blocking with 5% skim milk. Subsequent incubation with appropriate secondary antibodies and visualization of protein bands using ECL solution (Biosharp) were performed. The expression levels of target proteins were normalized to the housekeeping gene GAPDH.

Statistical analysis

All experiments were repeated at least 3 times, and data are presented as the mean ± standard deviation. Student's 2-tailed paired *t*-test was analyzed between 2 groups, and Analysis of Variance followed by the least significant differences method was used for 3 or more groups. All statistical analyses were used with SPSS 26.0 software (IBM).

Results

Microencapsulated 3D culture improved cell proliferation, and stemness of hUCMSCs

3D-hUCMSCs exhibited a spheroidal and homogeneous morphology, with hUCMSCs aggregating into spherical growth (Figure 1A). The apoptosis of 2D-hUCMSCs and 3D-hUCMSCs was compared by flow cytometry. The results showed that the apoptosis rate of 3D-hUCMSCs was comparable to that of 2D-hUCMSCs (Figure 2A). This indicates that microencapsulated 3D culture does not induce apoptosis in hUCMSCs. Subsequently, the expression of surface marker molecules of

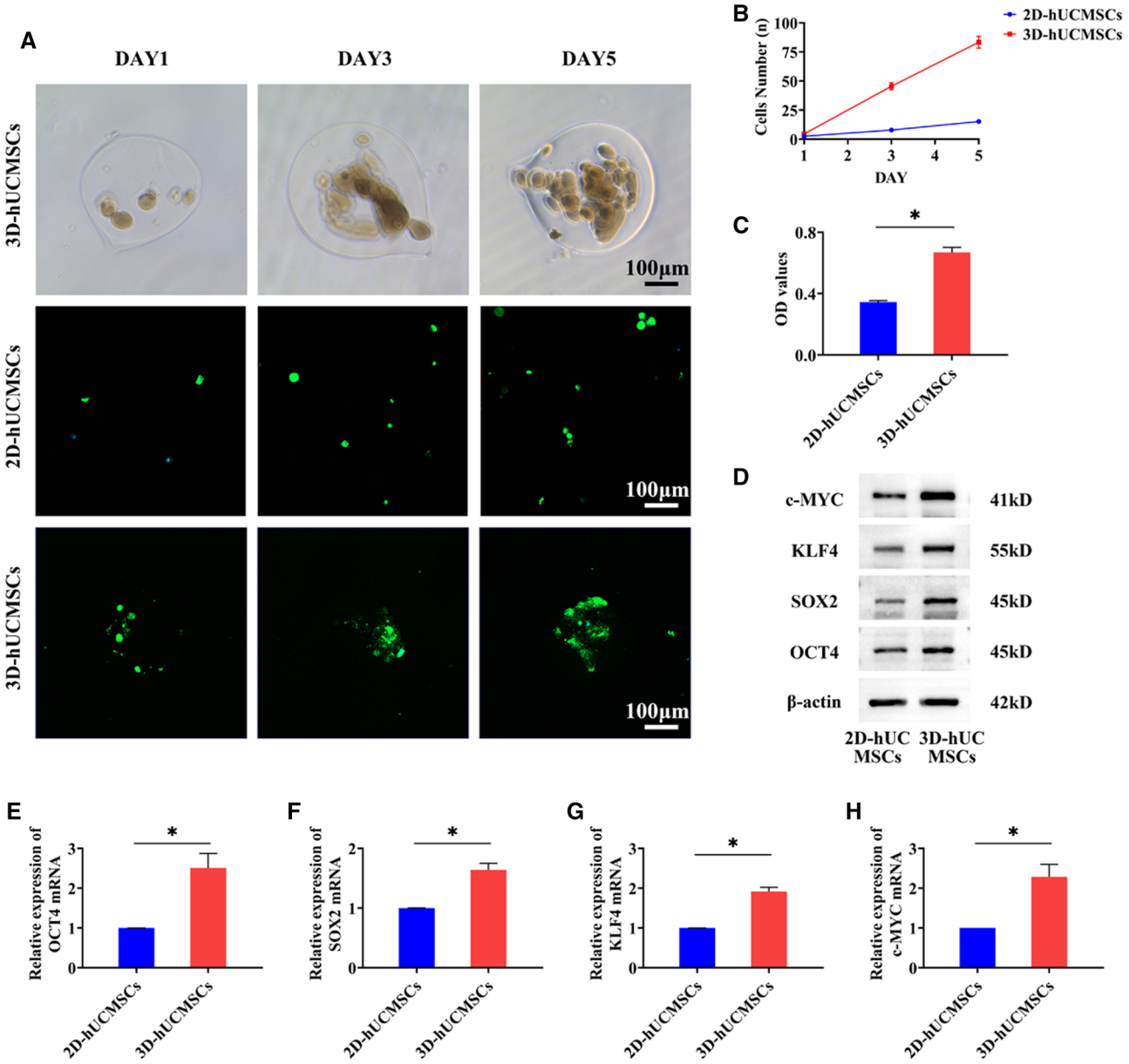

Figure 1. The cell proliferation and stemness of 3D-hUCMSCs. (A) Microscopic morphology of 3D-hUCMSCs. Scale bars: 100 μm. (B) Statistical analysis of cell counts on day 1, 3, and 5 of 3D-hUCMSCs. At least 6 representative visual fields for each were counted. (C) Proliferation of hUCMSCs detected by CCK8 ($n = 3$). (D) Western blot results of OCT4, SOX2, KLF4, and c-MYC. (E-H) Relative mRNA expression of OCT4, SOX2, KLF4, and c-MYC adjusted to GAPDH ($n = 3$). 3D-hUCMSCs, 3D culture of human umbilical cord-derived mesenchymal stem cells.

hUCMSCs after 3D microencapsulation culture was characterized by flow cytometry. As shown in Figure 2B, 3D-hUCMSCs were positive for CD90, CD73, and CD105, while negative for CD14, CD34, and CD45, which meet the criteria for hUCMSCs. In addition, the osteogenic, chondrogenic, and adipogenic differentiation potential of 3D-hUCMSCs was confirmed by differentiation-inducing medium assay (Figure 2C).

To compare the cell number, the hUCMSCs were stained with Ethidium Homodimer-1 and Hoechst and calculated the count of inner cell spheroid (Figure 1B). The 3D reconstruction of the inner cell spheroid was shown on day 1, day 3, and day 5 (Supplementary Files: S1-S3). The results showed that microencapsulated 3D culture significantly increased the cell count compared with 2D-hUCMSCs on day 3 (2D-hUCMSCs: 7.83 ± 3.251; 3D-hUCMSCs: 45.50 ± 7.477) and day 5 (2D-hUCMSCs: 15.17 ± 1.169; 3D-hUCMSCs: 83.33 ± 12.501). Furthermore, the cell proliferation of 3D-hUCMSCs was assessed using a CCK8 assay on day 5. The cell proliferation of 3D-hUCMSCs was significantly higher than that of 2D-hUCMSCs (Figure 1C). These findings suggest that microencapsulated 3D culture enhances the cell proliferation of hUCMSCs.

To investigate the effects of microencapsulated 3D culture on the properties of hUCMSCs, the expression of stem cell pluripotency transcription factors, OCT4, SOX2, KLF4, and c-MYC, was examined by western blot and qRT-PCR. Western blot results showed that protein expression levels of OCT4, SOX2, KLF4, and c-MYC were higher in 3D-hUCMSCs than in 2D-hUCMSCs (Figure 1D). qRT-PCR results demonstrated that mRNA expression levels of these pluripotency

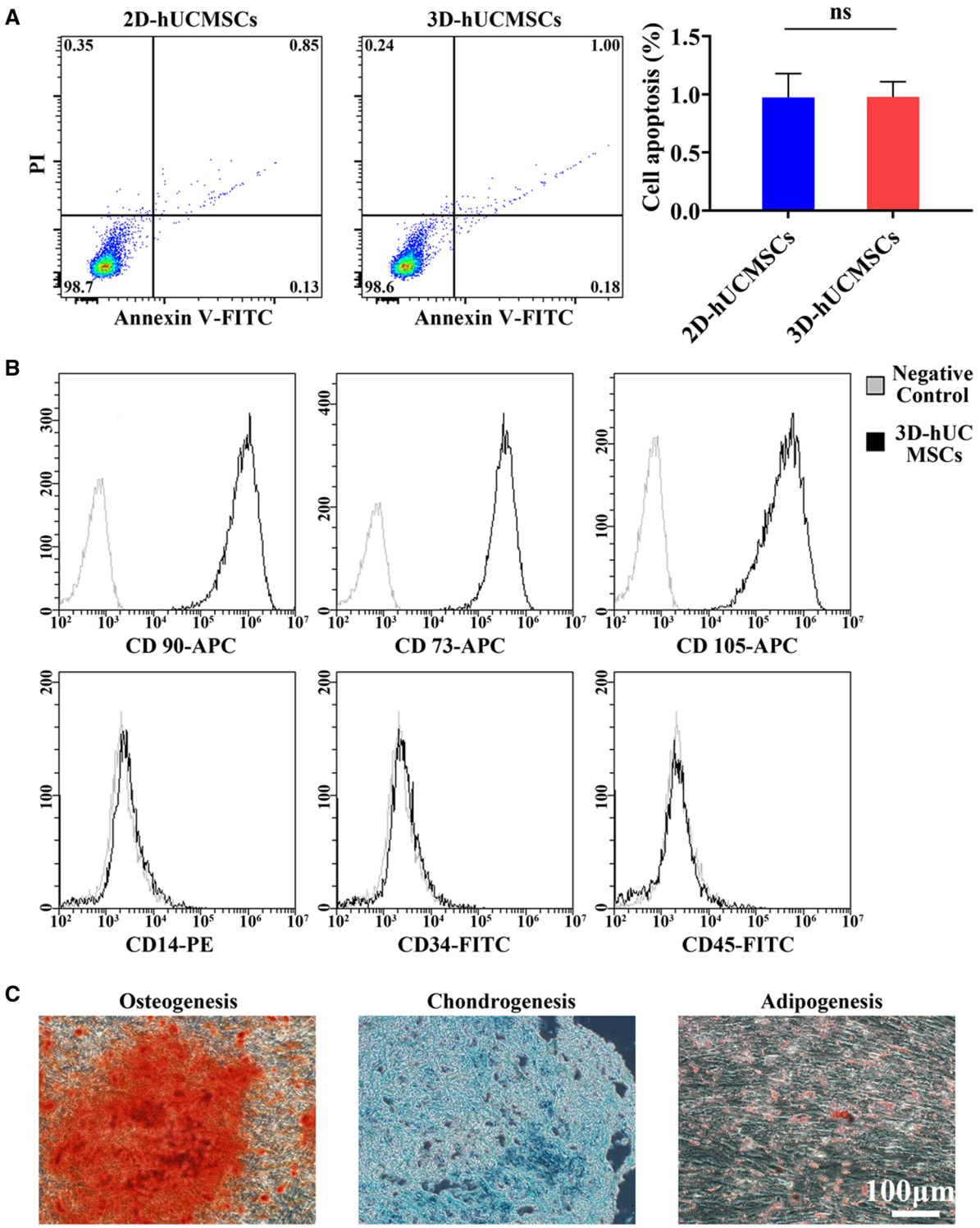

Figure 2. Phenotype of 3D-hUCMSCs. (A) The apoptosis of 2D-hUCMSCs (left) and 3D-hUCMSCs (center) was detected by flow cytometry and statistically analyzed in both groups (right). (B) 3D-hUCMSCs specific surface markers detected by flow cytometry. The grey lines represent the expression level of the negative control, and the black lines represent 3D-hUCMSCs. (C) Osteogenic, chondrogenic, and adipogenic induction of BMSCs at 21d. Scale bars: 100 μm. 3D-hUCMSCs, 3D culture of human umbilical cord-derived mesenchymal stem cells; BMSCs, bone marrow stem cells.

transcription factors were higher in 3D-hUCMSCs compared to 2D-hUCMSCs (OCT4: $P = .018785$; SOX2: $P = .000541$; KLF4: $P = .000116$; c-MYC: $P = .001975$) (Figure 1E-H). These results indicate that microencapsulated 3D culture enhances the stemness of hUCMSCs.

3D-hUCMSCs restored the damaged uterus

To evaluate the therapeutic efficacy in IUA model, 3D-hUCMSCs were injected via the tail vein to treat mice. The illustration of microencapsulated 3D culture and treatment timeline is shown in Figure 3A. In the Sham group, the uterus exhibited

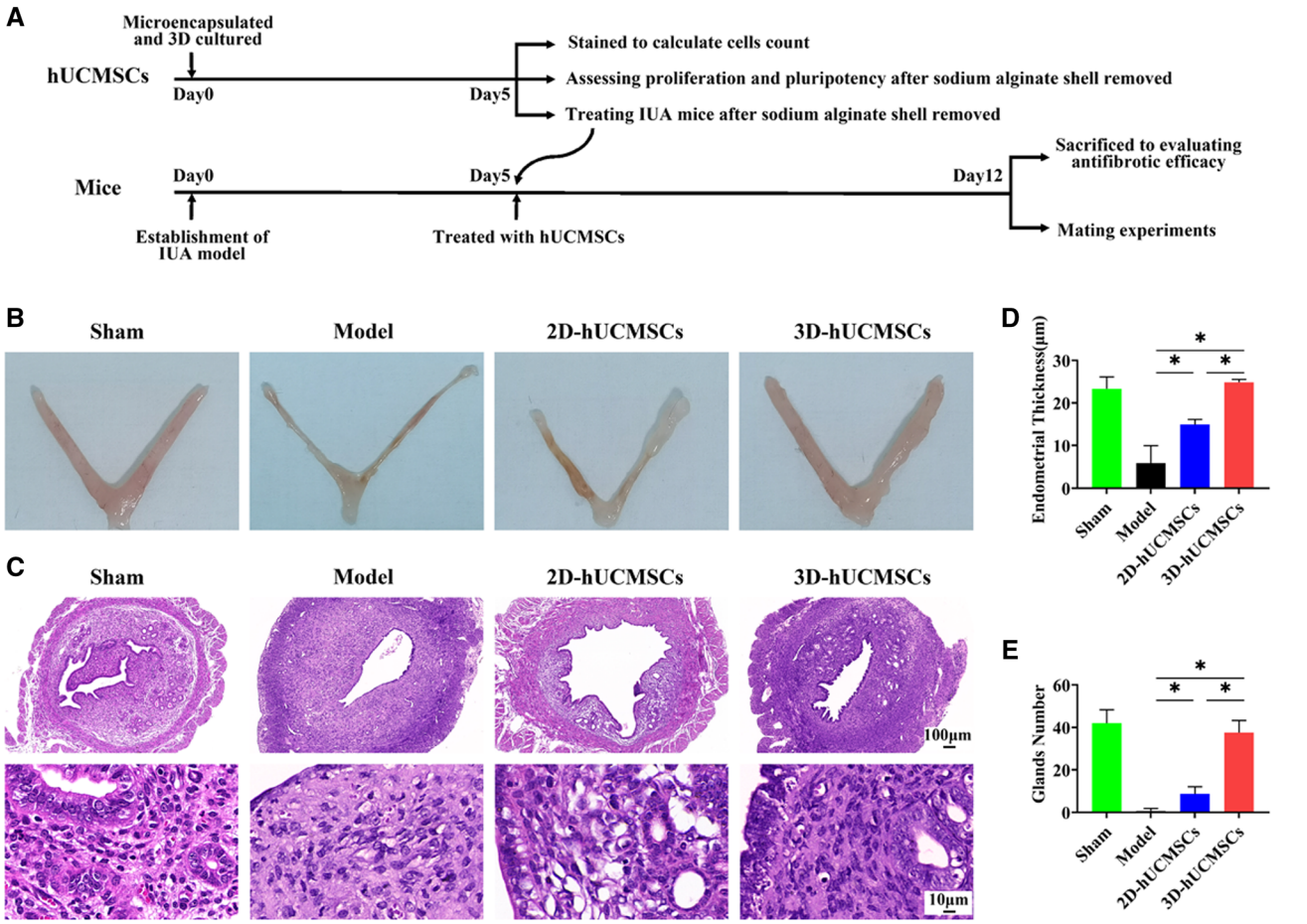

Figure 3. 3D-hUCMSCs restored the damaged uterine. (A) The illustration of microencapsulated 3D culture and treatment timeline. (B) The morphology of mice uterine after saline or hUCMCSs treatments. (C) H&E staining of mice uterine after different treatments. Scale bars: 100 μm (above), 10 μm (below). (D, E) Statistical analysis of the endometrial thickness and number of glands in each group ($n = 6$). 3D-hUCMSCs, 3D culture of human umbilical cord-derived mesenchymal stem cells; H&E, hematoxylin and eosin; UCMCSs, umbilical cord-derived mesenchymal stem cells

a full shape with regular edges. The Model group showed obvious narrowing and twisting of bilateral uterine horns, and some of them along with uterine fluid. The uterine horns in the 2D-hUCMSCs group displayed partial recovery, but some remained slender and tortuous. The uterine morphology in the 3D-hUCMSCs group closely resembled that of the Sham group (Figure 3B). Hematoxylin and eosin staining was performed to assess the endometrial recovery in 3D-hUCMSCs administration. In the Sham group, the endometrial structure was intact, with abundant interstitial glands and an integral monolayer of columnar epithelium on the uterine cavity surface. The Model group exhibited abnormal endometrial structure, with narrowed or atretic uterine cavities (Figure 3C). The endometrial thickness significantly decreased in the Model group (5.78 ± 4.155 mm) compared to the Sham group (23.33 ± 2.802 mm, $P < .0001$). Both the 2D-hUCMSCs group (14.89 ± 1.222 mm, $P < .0001$) and 3D-hUCMSCs group (24.86 ± 0.683 mm, $P < .0001$) showed an increase in endometrial thickness compared to the Model group, and endometrial thickness of the 3D-hUCMSCs group significantly more than 2D-hUCMSCs group ($P < .0001$) (Figure 3D). The number of glands increased in both the 2D-hUCMSCs group (8.67 ± 3.386, $P = .007$) and 3D-hUCMSCs group (37.5 ± 5.718, $P < .0001$) compared to the Model group (0.67 ± 1.211). The number of glands of the 3D-hUCMSCs group was also significantly more than the 2D-hUCMSCs group ($P < .0001$) (Figure 3E).

3D-hUCMSCs inhibited endometrial fibrosis and alleviated endometrial inflammation

The endometrial fibrosis was evaluated using Masson staining to assess the antifibrotic efficacy of 3D-hUCMSCs. The fibrous tissue area significantly increased in the Model group in comparison to the Sham group ($P < .0001$). The percentage of fibrotic area obviously decreased in 2D-hUCMSCs ($P < .0001$) and 3D-hUCMSCs ($P < .0001$) compared to the Model group. Moreover, the 3D-hUCMSCs group exhibited a significantly lower percentage of fibrotic area compared to the 2D-hUCMSCs group ($P < .0001$) (Figure 4A and D).

To further evaluate the level of fibrosis, we examined the expression of fibrosis factors, collagen I, and α-SMA, in the endometrium by immunohistochemistry. Immunohistochemical staining for collagen I indicated a significant increase in positive staining in the Model group compared to the Sham group ($P < .0001$). Both 2D-hUCMSCs group ($P < .0001$) and the 3D-hUCMSCs group ($P < .0001$) showed a decrease in collagen I expression compared to the Model group. Furthermore, the 3D-hUCMSCs group exhibited lower levels of collagen I expression than the 2D-hUCMSCs group ($P < .0001$) (Figure

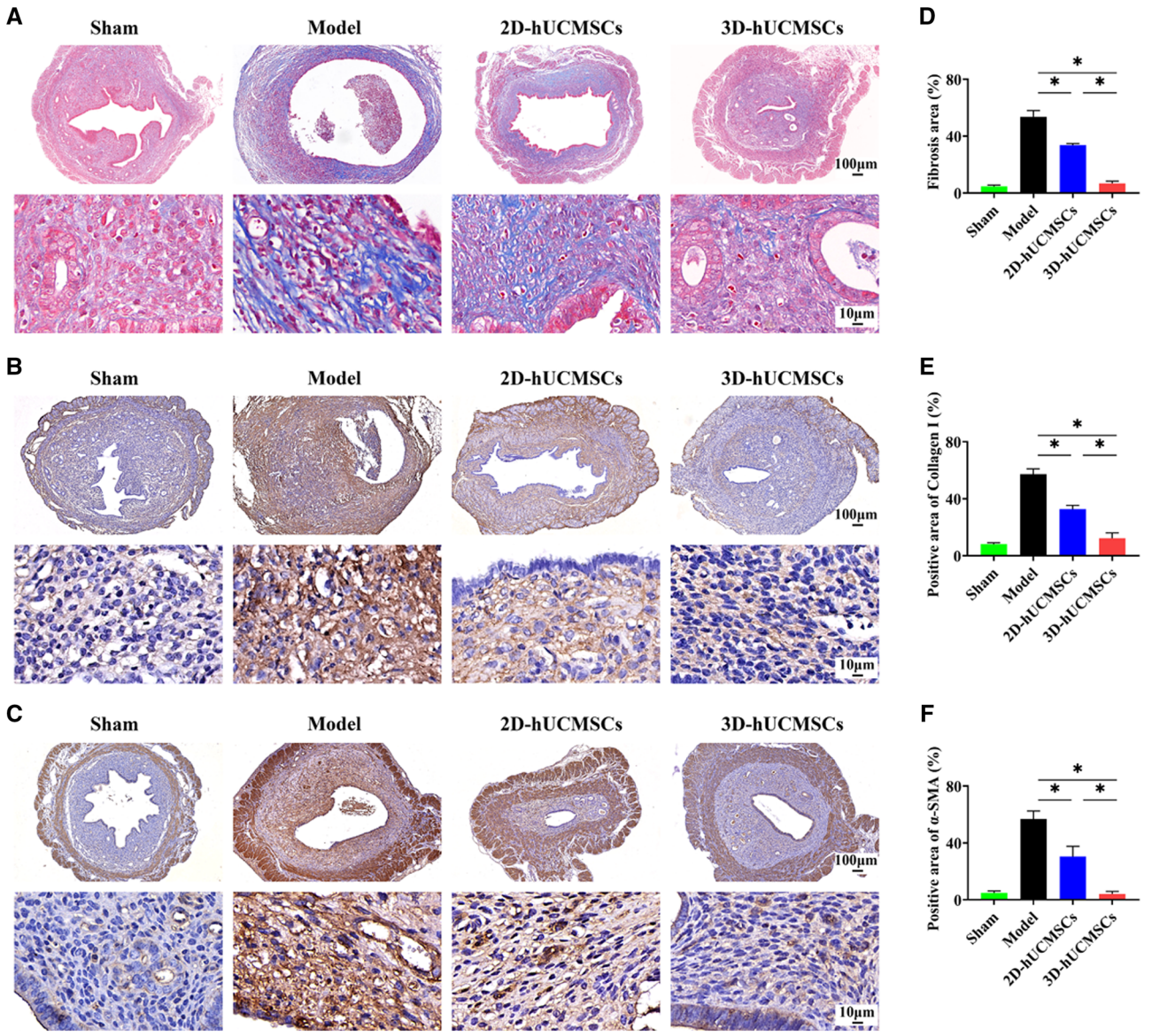

Figure 4. 3D-hUCMSCs ameliorated fibrosis of uterine tissue. (A) Masson staining of mice uterine after different treatments. Scale bars: 100 μm (above), 10 μm (below). (B, C) Immunohistochemical staining of collagen I and α-SMA. Scale bars: 100 μm (above), 10 μm (below). (D) Statistical analysis of the percentage of fibrosis area in each group ($n = 6$). (E, F) Statistical analysis of the percentage of collagen I, α-SMA-positive areas ($n = 6$). 3D-hUCMSCs, 3D culture of human umbilical cord-derived mesenchymal stem cells; α-SMA, α-smooth muscle actin.

4B and E). Expression of α-SMA was significantly increased in the Model group compared with the Sham group ($P < .0001$), but decreased in both the 2D-hUCMSCs ($P < .0001$) and 3D-hUCMSCs groups ($P < .0001$) compared with the Model group. The 3D-hUCMSCs group displayed significantly lower α-SMA expression than the 2D-hUCMSCs group ($P < .0001$) (Figure 4C and F).

The expression of pro-inflammatory factors was detected by ELISA and qRT-PCR to assess the level of endometrial inflammation (Figure 5A-D). Compared to those in the Sham group, the protein and mRNA levels of TNF-α (protein: $P < .0001$; mRNA: $P < .0001$) and IL-1 (protein: $P < .0001$; mRNA: $P < .0001$) showed a significant increase in the Model group. After treatment with 2D-hUCMSCs (TNF-α protein: $P < .0001$; TNF-α mRNA: $P < .0001$; IL-1 protein: $P = .0497$; IL-1 mRNA: $P < .0001$) and 3D-hUCMSCs (TNF-α protein: $P < .0001$; TNF-α mRNA: $P < .0001$; IL-1 protein: $P < .0001$; IL-1 mRNA: $P < .0001$), the expression levels of TNF-α and IL-1 were remarkably decreased. And the 3D-hUCMSCs group exhibited lower levels of pro-inflammatory factors than the 2D-hUCMSCs group (TNF-α protein: $P < .0001$; TNF-α mRNA: $P = .0003$; IL-1 protein: $P = .0006$; IL-1 mRNA: $P < .0001$). This suggests that 3D-hUCMSCs can alleviate endometrial inflammation in IUA mice.

3D-hUCMSCs inhibited the TGF-β1/Smad3 signaling pathway

To determine whether the TGF-β1/Smad3 pathway was involved in the inhibition of endometrial fibrosis by 3D-hUCMSCs, western blot and qRT-PCR were employed to assess protein and mRNA expression of TGF-β1, Smad3. In the Model group, the protein expressions of TGF-β1, Smad3, and p-Smad3 were significantly higher than that of the Sham group, as were the expression levels of TGF-β1 mRNA ($P < .0001$) and Smad3

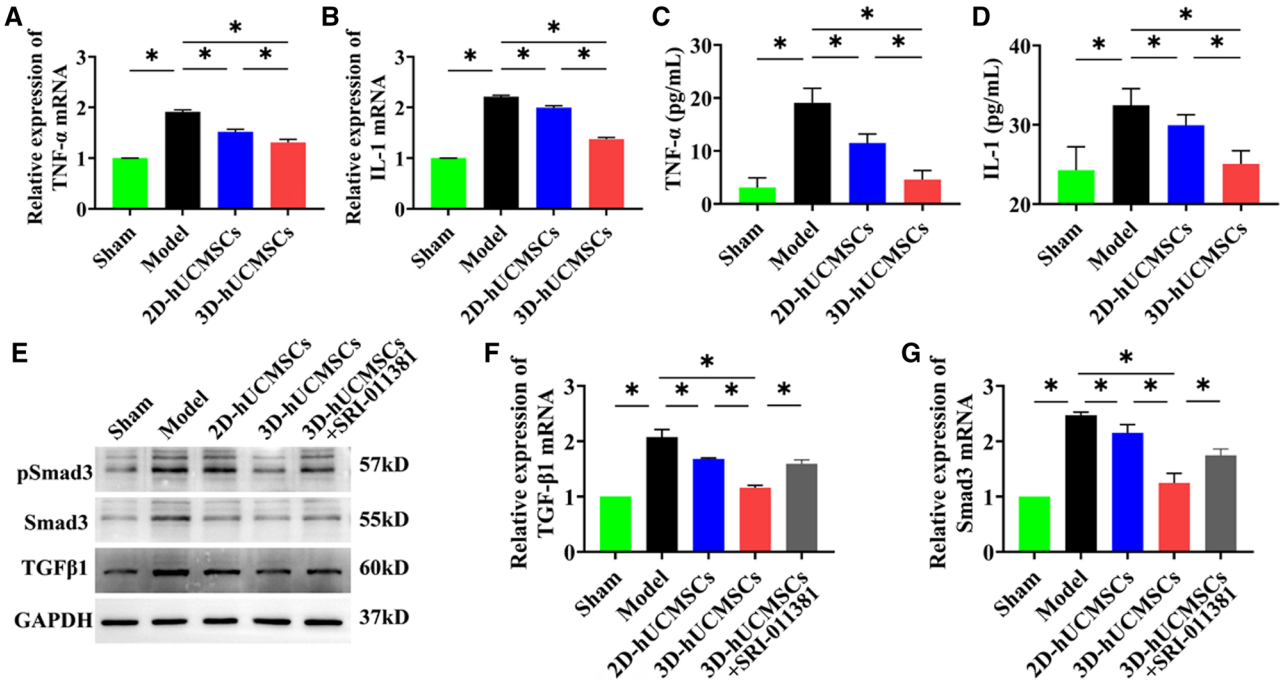

Figure 5. 3D-hUCMSCs inhibited inflammation and the TGF-β1/Smad3 pathway. (A, B) The protein expression of TNF-α and IL-1 detected by ELISA ($n = 6$). (C, D) Relative mRNA expression of TNF-α and IL-1 ($n = 3$). (E) Western blot results of TGF-β1, Smad3, and pSmad3. (F, G) Relative mRNA expression of TGF-β1 and Smad3 ($n = 3$). 3D-hUCMSCs, 3D culture of human umbilical cord-derived mesenchymal stem cells; IL-1, interleukon-1; TNF-α, tumor necrosis factor alpha.

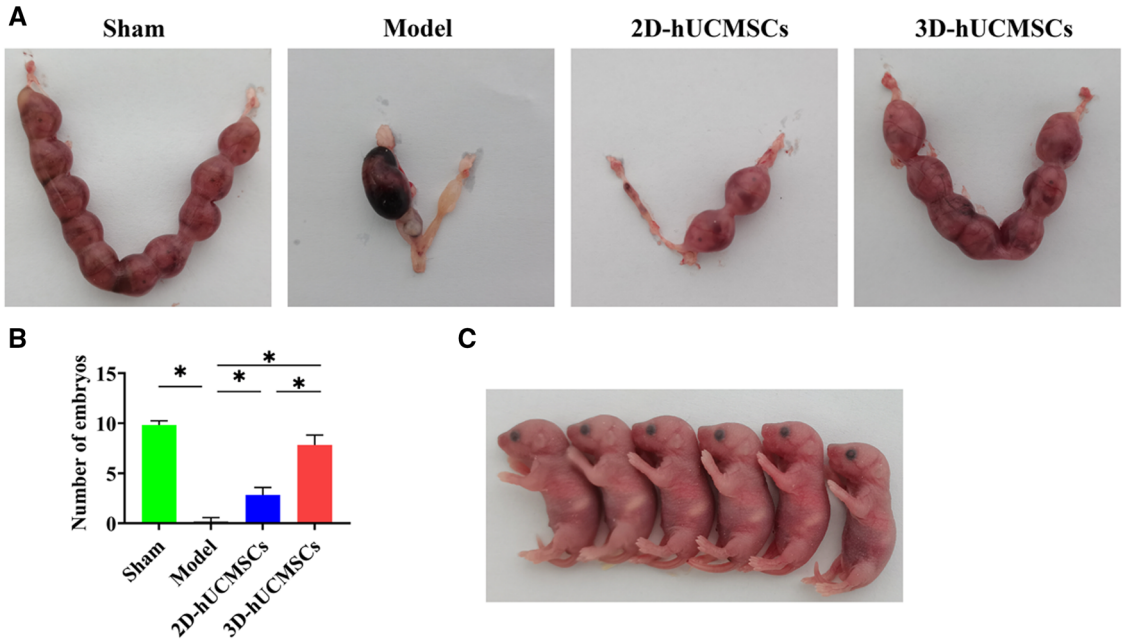

Figure 6. 3D-hUCMSCs improved fertility restoration. (A) The uterine appearance of mice on day 10.5 of pregnancy after different treatments. (B) Statistical analysis of the implantation embryo numbers ($n = 6$). (C) The newborn mice in the 3D-hUCMSCs group. 3D-hUCMSCs, 3D culture of human umbilical cord-derived mesenchymal stem cells.

mRNA ($P < .0001$), indicating activation of the TGF-β1/Smad3 signaling pathway (Figure 5E-G). The 2D-hUCMSCs and 3D-hUCMSCs groups exhibited lower protein expressions of TGF-β1, Smad3, and pSmad3 compared to the Model group. Additionally, mRNA expressions of TGF-β1 and Smad3 were lower in the 2D-hUCMSCs group (TGF-β1 mRNA: $P = .000512$; Smad3 mRNA: $P = .000763$) and 3D-hUCMSCs group (TGF-β1 mRNA: $P < .0001$; Smad3 mRNA: $P < .0001$) than that of the Model group (Figure 5F and G). The 3D-hUCMSCs group demonstrated a lower expression level of the TGF-β1/Smad3 pathway compared to the 2D-hUCMSCs group. To further explore the effects of 3D-hUCMSCs on the TGFβ1/Smad signaling pathway, we intervened with the pathway agonist SRI-011381 in a group named 3D-hUCMSCs+SRI-011381

group: after 3D-hUCMSCs treatment, SRI-011381 (MCE, China), solubilized in saline containing Dimethyl Sulfoxide (10%) and PEG300 (40%), was injected intraperitoneally into mice at a dose of 30 mg/kg every 2 days.[29,30] Subsequently, uterine tissue was collected to extract protein and mRNA. Both western blot and qRT-PCR results showed that SRI-011381 significantly reversed the suppression of the TGF-β1/Smad3 pathway by 3D-hUCMSCs (Figure 5E-G). These results suggest that 3D-hUCMSCs more effectively inhibited the activation of the TGF-β1/Smad3 signaling pathway in the mouse uterus.

3D-hUCMSCs restored the fertility in the IUA model

Endometrial function was evaluated through a mating experiment, with mice sacrificed at 10.5 days of gestation. Macroscopic examination revealed bilaterally symmetrical uterine horns and similarly sized embryos in the Sham group. In the Model group (0.17 ± 0.167), the number of embryos was significantly lower compared to the Sham group (9.83 ± 0.408, $P < .0001$), with notable fluid accumulation in some uterine cavities. The total number of embryos per mouse in the 2D-hUCMSCs group (2.83 ± 0.753, $P < .0001$) was higher than that in the Model group but significantly lower than that in the 3D-hUCMSCs group (7.83 ± 0.983, $P < .0001$) (Figure 6A and B). In addition, no tumor formation was observed in any of the hUCMSCs-treated mice in this study. And the newborn mice in the 3D-hUCMSCs group had no obvious malformations (Figure 6C).

Discussion

The potential of MSCs in cell-based therapeutic applications has been recognized due to their multipotent differentiation capabilities and immunomodulatory characteristics. There is an urgent need for a large quantity of high-quality MSCs for clinical treatments. However, conventional 2D cultured MSCs are greatly limited in cell amount and proliferation. In this study, our findings demonstrated that microencapsulated 3D culture significantly augmented the quantity, cell proliferation, and stemness of hUCMSCs. 3D-hUCMSCs promoted the recovery of endometrial morphology and function, and decreased the expression of the TGF-β1/Smad3 pathway in the mouse endometrium, contributing to the effective alleviation of endometrial fibrosis.

The growth and function of MSCs are intricately tied to interactions with surrounding cells or the extracellular matrix.[31] In their native tissue microenvironments, MSCs typically aggregate with neighboring MSCs or various other cells, forming spheroids that facilitate extensive cell-to-cell and cell-to-microenvironment interactions.[31] Under conventional 2D conditions, the proliferation and growth of MSCs are compromised due to the altered association between MSCs and their microenvironment. In order to achieve the required quantity of cells for clinical therapy, the culture duration needs to be extended.[32] However, prolonged cultivation of MSCs under 2D conditions has been associated with the accumulation of chromosomal aberrations, attributed to the altered interaction between MSCs and their microenvironment.[33] Furthermore, substantial evidence indicates that long-term 2D culture leads to a loss of MSC pluripotency.[34] Consequently, many studies advocate for the use of 3D sphere culture for MSCs. In vitro MSC spheroid culture has been shown to enhance the production of extracellular matrix within the spheroids, thereby promoting increased cell-cell and cell-matrix interactions.[35–37] The cell morphology, viability, and senescence of 3D spheroid-cultured Wharton's jelly mesenchymal stem cells (WJ-MSCs) were comparable to their 2D-cultured counterparts. However, the expression of pluripotency markers (OCT4, SOX2, and NANOG) was 2-8 times higher in 3D spheroid-cultured WJ-MSCs.[20] Various 3D sphere culture methods were employed for MSCs, such as 3D microtiter, hanging drop, and ultralow attachment plate-based spheroid culture.[19,20] However, these 3D spheroid culture methods are not suitable for the long-term culture of MSCs and their local application in the uterine cavity.

To address the challenges, many biomaterials have been utilized to construct scaffolds, which provide a 3D environment conducive to the growth of MSC and the enhancement of their regenerative repair capabilities.[38] These biomaterial scaffolds also function as vehicles for the transportation of MSCs into the uterine cavity, thereby prolonging their retention period and augmenting their bioavailability. The composite hydrogel could encapsulate MSCs and extend the release time to more than 7 days.[39] However, these materials often serve as carriers to provide vehicles for MSCs. The large quantity of high-quality MSCs remains a challenge. Moreover, the impact of these materials on the cellular properties of MSCs, including cell differentiation and pluripotency, continues to be a contentious topic.

In response to these challenges, we developed the microencapsulated 3D culture for MSCs. This method involves the encapsulation of human umbilical cord-derived mesenchymal stem cells (hUCMSCs) and collagen, constituting the core of the microcapsules, within a sodium alginate solution to form microsphere capsules under high-voltage electrostatic conditions. Sodium alginate, acknowledged for its superior biocompatibility, cost-effectiveness, and proficiency in drug encapsulation, was employed as the encapsulating material. The microencapsulation shells not only facilitated the exchange of nutrients and metabolites but also provided protection to the encapsulated cells from external stress damage and immune rejection.[40] Collagen, a component of the extracellular matrix, offered good biocompatibility and the ability to mimic the extracellular matrix of MSCs, thereby regulating their growth and function.[41–43] The microencapsulated 3D culture technique enabled the formation of MSC spheroids, allowing for extended in vitro cultivation. Furthermore, the microencapsulated 3D culture technique could generate large quantities of MSCs, and is both cost-effective and straightforward to implement.

This study primarily focused on the influence of the microencapsulated 3D culture method on the characteristics and efficacy of hUCMSCs. By staining and enumerating the nuclei of hUCMSCs on days 1, 3, and 5 of the 3D microencapsulated culture, we observed a significant increase in the cell count of hUCMSCs. On the fifth day of microencapsulated 3D culture, the hydrogel shells were removed to investigate the effects of this 3D culture on the cell proliferation and stemness of hUCMSCs. CCK-8 results indicated that microencapsulated 3D culture could improve the cell proliferation of hUCMSCs. We observed a significant upregulation in the expression of these stemness genes, such as OCT4, SOX2, KLF4, and c-MYC, in hUCMSCs after 3D microencapsulated culture. These findings suggest that microencapsulated 3D culture enhances the stemness of hUCMSCs.

The endometrium in the Model group exhibited abnormal morphology, characterized by epithelial thinning on the surface of the uterine cavity, diminished gland numbers, increased fibrotic areas, and reduced pregnancy rates. After tail vein injection, 3D-hUCMSCs improved the endometrial morphology, increased endometrial thickness and gland numbers, and inhibited the fibrosis. Notably, the improvement in endometrial morphology was more pronounced with hUCMSCs subjected to microencapsulated 3D culture compared to conventionally cultured hUCMSCs. Mating experiments further supported the superior ability of 3D-hUCMSCs to promote endometrial function recovery. These findings suggest that the microencapsulated 3D culture enhances the intrinsic function of hUCMSCs in promoting morphological and functional repair of the endometrium. No obvious malformations were found in newborn mice of 3D-hUCMSCs group, and no tumor formation was observed in hUCMSCs-treated mice, which preliminarily verified the safety of 3D-hUCMSCs treatment.

Fibrosis following injury to the endometrial basal layer could lead to partial or total IUA, rendering the inhibition of fibrosis crucial for IUA treatment.[44] TGF-β1, a classic pro-inflammation and fibrosis cytokine, is associated with numerous biological processes, including inflammatory activity, cell adhesion, and fibrosis progress. The TGF-β1/Smad3 signaling pathway has been implicated in various fibrotic disorders, playing a significant role in the development of IUA.[45–47] Transforming growth factor beta 1 activates downstream signaling through Smad3, leading to excessive deposition of extracellular matrix components such as α-SMA and collagen I, and contributing to tissue fibrosis formation.[48–50] The results demonstrated a significant increase in the expression of TGF-β1, Smad3, and pSmad3 in the Model group, indicating activation of the TGF-β1/Smad3 signaling pathway. While hUCMSCs effectively reversed this activation, 3D-hUCMSCs exerted the potent effects. In addition, agonist SRI-011381 attenuated the inhibitory effect of 3D-hUCMSCs on TGF-β1/Smad3 signaling pathway. Evaluation of endometrial fibrosis through Masson staining and the detection of α-SMA and collagen I expression revealed that hUCMSCs significantly reduced the area of fibrosis and decreased the expression of α-SMA and collagen I. This suggests that hUCMSCs decreased the α-SMA and collagen I expression via inhibiting the TGF-β1/Smad3 signaling pathway, and 3D-hUCMSCs exhibited a stronger antifibrotic effect. In conclusion, the microencapsulated 3D culture enhanced the antifibrotic effect of hUCMSCs through the TGF-β1/Smad3 signaling pathway.

Infection and inflammatory exudates following endometrial injury are recognized as important risk factors for the occurrence of IUA.[44] After severe damage to the basal layer, numerous fibroblasts and inflammatory cells accumulate in the damaged endometrium, secreting a variety of inflammatory mediators and inducing an inflammatory response.[51] Especially, they secrete pro-inflammatory factors such as TNF-α and IL-1β, which in turn promote the development of IUA.[51,52] In this study, our experimental results showed that the protein and mRNA levels of TNF-α and IL-1β were significantly elevated in the Model group mice. Whereas their levels were significantly reduced after hUCMSCs treatment, especially 3D-hUCMSCs treatment. This result suggests that 3D-hUCMSCs can reduce the release of pro-inflammatory factors after endometrial injury and thus have a protective effect against IUA.

In this study, we employed 3D microencapsulated culture to facilitate the long-term culture of hUCMSCs in vitro, which distinguished by its operational simplicity, scalability, and biocompatibility, provides ample growth space for hUCMSCs in a spherical shape. The microencapsulated shells act as a protective barrier, reducing external mechanical stress damage to hUCMSCs. We removed the microencapsulated shells and explored the effects of 3D culture on the characteristics and therapeutic efficacy of hUCMSCs. We found that this microencapsulated 3D culture significantly enhanced the amount, proliferation, and stemness of hUCMSCs, and we also verified the promotional effects of microencapsulated 3D culture on the anti-inflammatory and anti-fibrotic properties of hUCMSCs in IUA mice. Regrettably, our current study remains at the animal level, necessitating further exploration for the safety and efficacy of microencapsulated 3D-hUCMSCs in clinical research. Meanwhile, we will further explore the relevant mechanisms of microencapsulated 3D culture to improve cell proliferation and stemness of hUCMSCs.

Conclusion

In conclusion, our study demonstrates the therapeutic capabilities of 3D-hUCMSCs in treating IUA. Notably, microencapsulated 3D culture enhances the cell proliferation and stemness of hUCMSCs, exerting more pronounced antifibrotic and anti-inflammatory effects. Furthermore, 3D-hUCMSCs contribute significantly to endometrial regeneration through the inhibition of the TGF-β1/Smad3 signaling pathway. These findings provide a valuable approach for treating IUA and establish a foundation for the clinical application of hUCMSCs.

Acknowledgements

Not applicable.

Author contributions

Hongjiang Liu (Data curation, Formal analysis, Investigation, Methodology, Project administration, Visualization, Writing -original draft, Writing-review & editing), Xiaohua Jiang (Funding acquisition, Formal analysis, Investigation, Methodology, Project administration, Validation, Writing-review & editing), Jin Qian (Investigation, Methodology, Resources, Methodology, Validation, Visualization, Writing-review & editing), Xuan Xu (Investigation, Resources, Validation), Shujun Yu (Resources, Validation), Zhongqin Tang (Data curation, Validation), Ying Wang (Data curation, Resources), Qiong Xing (Resources, Validation), Heng Tang (Conceptualization, Methodology, Supervision, Resources), Jianye Wang (Conceptualization, Funding acquisition, Methodology, Resources, Supervision), and Zhaolian Wei (Conceptualization, Funding acquisition, Methodology, Project administration, Supervision, Writing-review & editing)

Supplementary material

Supplementary material is available at *Stem Cells Translational Medicine* online.

Funding

This work was supported by National Natural Science Foundation of China (No. 82171619), Anhui Provincial Natural Science Foundation for Universities (No. 2022AH051193), and Anhui Provincial Institute of Translational Medicine (No. 2023zhyx-C54).

Conflicts of interest

The authors declare that they have no competing interests.

Data availability

The data underlying this article will be shared on reasonable request to the corresponding author.

Ethics approval and consent to participate

This study has been approved by the Animal Ethics Committee of Anhui Medical University (Title: Study on the effect and mechanism of hydrogel microencapsulated MSCs to inhibit intrauterine adhesion by enhancing miR-219-5p in exosomes; No. 20210862; Date of approval: March 1, 2021).

Consent for publication

Not applicable.

References

[1]. Yu D, Wong Y-M, Cheong Y, et al. Asherman syndrome—one century later. *Fertil Steril*. 2008;89:759-779.
[2]. Dreisler E, Kjer JJ. Asherman's syndrome: current perspectives on diagnosis and management. *Int J Womens Health*. 2019;11:191-198.
[3]. Ma J, Zhan H, Li W, et al. Recent trends in therapeutic strategies for repairing endometrial tissue in intrauterine adhesion. *Biomater Res*. 2021;25:40.
[4]. Liu T, He B, Xu X. Repairing and regenerating injured endometrium methods. *Reprod Sci*. 2023;30:1724-1736.
[5]. Li J, Pan Y, Yang J, et al. Tumor necrosis factor-α-primed mesenchymal stem cell-derived exosomes promote M2 macrophage polarization via galectin-1 and modify intrauterine adhesion on a novel murine model. *Front Immunol*. 2022;13:945234.
[6]. Tang PM, Nikolic-Paterson DJ, Lan HY. Macrophages: versatile players in renal inflammation and fibrosis. *Nat Rev Nephrol*. 2019;15:144-158.
[7]. Geng XQ, Ma A, He JZ, et al. Ganoderic acid hinders renal fibrosis via suppressing the TGF-beta/Smad and MAPK signaling pathways. *Acta Pharmacol Sin*. 2020;41:670-677.
[8]. Brown C, Mckee C, Bakshi S, et al. Mesenchymal stem cells: cell therapy and regeneration potential. *J Tissue Eng Regen Med*. 2019;13:1738-1755.
[9]. Lee W-L, Liu C-H, Cheng M, et al. Focus on the primary prevention of intrauterine adhesions: current concept and vision. *Int J Mol Sci*. 2021;22:5175.
[10]. Benor A, Gay S, Decherney A. An update on stem cell therapy for asherman syndrome. *J Assist Reprod Genet*. 2020;37:1511-1529.
[11]. Meng X, Ichim TE, Zhong J, et al. Endometrial regenerative cells: a novel stem cell population. *J Transl Med*. 2007;5:57.
[12]. Zhang L, Li Y, Dong Y-C, et al. Transplantation of umbilical cord-derived mesenchymal stem cells promotes the recovery of thin endometrium in rats. *Sci Rep*. 2022;12:412.
[13]. Qin W, Wang J, Hu Q, et al. Melatonin-pretreated human umbilical cord mesenchymal stem cells improved endometrium regeneration and fertility recovery through macrophage immunomodulation in rats with intrauterine adhesions. *Biol Reprod*. 2023;109:918-937.
[14]. Yao S, Zhou Z, Wang L, et al. Targeting endometrial inflammation in intrauterine adhesion ameliorates endometrial fibrosis by priming MSCs to secrete C1INH. *iScience*. 2023;26:107201.
[15]. Wong KU, Zhang A, Akhavan B, et al. Biomimetic culture strategies for the clinical expansion of mesenchymal stromal cells. *ACS Biomater Sci Eng*. 2023;9:3742-3759.
[16]. Knight E, Przyborski S. Advances in 3D cell culture technologies enabling tissue-like structures to be created in vitro. *J Anat*. 2015;227:746-756.
[17]. Han M, Yang H, Lu X, et al. Three-dimensional-cultured MSC-derived exosome-hydrogel hybrid microneedle array patch for spinal cord repair. *Nano Lett*. 2022;22:6391-6401.
[18]. Wan X, Wu X, Hill MA, et al. ReN VM spheroids in matrix: a neural progenitor three-dimensional in vitro model reveals DYRK1A inhibitors as potential regulators of radio-sensitivity. *Biochem Biophys Res Commun*. 2020;531:535-542.
[19]. Jauković A, Abadjieva D, Trivanović D, et al. Specificity of 3D MSC spheroids microenvironment: impact on MSC behavior and properties. *Stem Cell Rev Rep*. 2020;16:853-875.
[20]. Thakur G, Bok E-Y, Kim S-B, et al. Scaffold-free 3D culturing enhance pluripotency, immunomodulatory factors, and differentiation potential of Wharton's jelly-mesenchymal stem cells. *Eur J Cell Biol*. 2022;101:151245.
[21]. Huang J, Li Q, Yuan X, et al. Intrauterine infusion of clinically graded human umbilical cord-derived mesenchymal stem cells for the treatment of poor healing after uterine injury: a phase I clinical trial. *Stem Cell Res Ther*. 2022;13:85.
[22]. Liu F, Hu S, Yang H, et al. Hyaluronic acid hydrogel integrated with mesenchymal stem cell-secretome to treat endometrial injury in a rat model of Asherman's syndrome. *Adv Healthc Mater*. 2019;8:e1900411.
[23]. Zhang Y, Shi L, Lin X, et al. Unresponsive thin endometrium caused by Asherman syndrome treated with umbilical cord mesenchymal stem cells on collagen scaffolds: a pilot study. *Stem Cell Res Ther*. 2021;12:420.
[24]. Li P, Fu L, Liao Z, et al. Chitosan hydrogel/3D-printed poly(ε-caprolactone) hybrid scaffold containing synovial mesenchymal stem cells for cartilage regeneration based on tetrahedral framework nucleic acid recruitment. *Biomaterials*. 2021;278:121131.
[25]. Zheng J-H, Zhang J-K, Kong D-S, et al. Quantification of the CM-Dil-labeled human umbilical cord mesenchymal stem cells migrated to the dual injured uterus in SD rat. *Stem Cell Res Ther*. 2020;11:280.
[26]. Zhao S, Agarwal P, Rao W, et al. Coaxial electrospray of liquid core–hydrogel shell microcapsules for encapsulation and miniaturized 3D culture of pluripotent stem cells. *Integr Biol (Camb)*. 2014;6:874-884.
[27]. Li J, Huang B, Dong L, et al. WJ-MSCs intervention may relieve intrauterine adhesions in female rats via TGFβ-1-mediated rho/ROCK signaling inhibition. *Mol Med Rep*. 2021;23:8.
[28]. Zhang L, Li Y, Guan CY, et al. Therapeutic effect of human umbilical cord-derived mesenchymal stem cells on injured rat endometrium during its chronic phase. *Stem Cell Res Ther*. 2018;9:36.
[29]. Wu Q, Miao X, Zhang J, et al. Astrocytic YAP protects the optic nerve and retina in an experimental autoimmune encephalomyelitis model through TGF-beta signaling. *Theranostics*. 2021;11:8480-8499.
[30]. Ren Y, Wu Y, He W, et al. SMOC2 plays a role in heart failure via regulating TGF-beta1/Smad3 pathway-mediated autophagy. *Open Med (Wars)*. 2023;18:20230752.
[31]. Kusuma GD, Li A, Zhu D, et al. Effect of 2D and 3D culture microenvironments on mesenchymal stem cell-derived extracellular vesicles potencies. *Front Cell Dev Biol*. 2022;10:819726.

[32]. Nikolits I, Nebel S, Egger D, et al. Towards physiologic culture approaches to improve standard cultivation of mesenchymal stem cells. *Cells*. 2021;10:886.
[33]. Ben-David U, Mayshar Y, Benvenisty N. Large-Scale analysis reveals acquisition of lineage-specific chromosomal aberrations in human adult stem cells. *Cell Stem Cell*. 2011;9:97-102.
[34]. Turinetto V, Vitale E, Giachino C. Senescence in human mesenchymal stem cells: functional changes and implications in stem cell-based therapy. *Int J Mol Sci*. 2016;17:1164.
[35]. Hu X, Xia Z, Cai K. Recent advances in 3D hydrogel culture systems for mesenchymal stem cell-based therapy and cell behavior regulation. *J Mater Chem B*. 2022;10:1486-1507.
[36]. Gilkes DM, Bajpai S, Chaturvedi P, et al. Hypoxia-inducible factor 1 (HIF-1) promotes extracellular matrix remodeling under hypoxic conditions by inducing P4HA1, P4HA2, and PLOD2 expression in fibroblasts. *J Biol Chem*. 2023;299:105144-110829.
[37]. Jorgenson AJ, Choi KM, Sicard D, et al. TAZ activation drives fibroblast spheroid growth, expression of profibrotic paracrine signals, and context-dependent ECM gene expression. *Am J Physiol Cell Physiol*. 2017;312:C277-C285.
[38]. Xiao B, Yang W, Lei D, et al. PGS scaffolds promote the In vivo survival and directional differentiation of bone marrow mesenchymal stem cells restoring the morphology and function of wounded rat uterus. *Adv Healthc Mater*. 2019;8:e1801455.
[39]. Feng M, Hu S, Qin W, et al. Bioprinting of a blue Light-Cross-Linked biodegradable hydrogel encapsulating amniotic mesenchymal stem cells for intrauterine adhesion prevention. *ACS Omega*. 2021;6:23067-23075.
[40]. Rastogi P, Kandasubramanian B. Review of alginate-based hydrogel bioprinting for application in tissue engineering. *Biofabrication*. 2019;11:042001.
[41]. Willershausen I, Barbeck M, Boehm N, et al. Non-cross-linked collagen type I/III materials enhance cell proliferation: in vitro and in vivo evidence. *J Appl Oral Sci*. 2014;22:29-37.
[42]. Wittig O, Diaz-Solano D, Cardier J. Viability and functionality of mesenchymal stromal cells loaded on collagen microspheres and incorporated into plasma clots for orthopaedic application: effect of storage conditions. *Injury*. 2018;49:1052-1057.
[43]. Nguyen TU, Watkins KE, Kishore V. Photochemically crosslinked cell-laden methacrylated collagen hydrogels with high cell viability and functionality. *J Biomed Mater Res A*. 2019;107:1541-1550.
[44]. Li X, Lv HF, Zhao R, et al. Recent developments in bio-scaffold materials as delivery strategies for therapeutics for endometrium regeneration. *Materials Today Bio*. 2021;11:100101.
[45]. Abudukeyoumu A, Li MQ, Xie F. Transforming growth factor-β1 in intrauterine adhesion. *Am J Rep Immunol*. 2020;84:e13262.
[46]. Lodyga M, Hinz B. TGF-β1—a truly transforming growth factor in fibrosis and immunity. *Semin Cell Dev Biol*. 2020;101:123-139.
[47]. De Oliveira RC, Wilson SE. Fibrocytes, wound healing, and corneal fibrosis. *Invest Opthalmol Vis Sci*. 2020;61:28.
[48]. Yao Y, Chen R, Wang G, et al. Exosomes derived from mesenchymal stem cells reverse EMT via TGF-β1/smad pathway and promote repair of damaged endometrium. *Stem Cell Res Ther*. 2019;10:225.
[49]. Yue Y, Meng K, Pu Y, et al. Transforming growth factor beta (TGF-β) mediates cardiac fibrosis and induces diabetic cardiomyopathy. *Diabetes Res Clin Pract*. 2017;133:124-130.
[50]. Huang C, Jing X, Wu Q, et al. Novel pectin-like polysaccharide from panax notoginseng attenuates renal tubular cells fibrogenesis induced by TGF-β. *Carbohydr Polym*. 2022;276:118772.
[51]. Lagana AS, Garzon S, Gotte M, et al. The pathogenesis of endometriosis: molecular and cell biology insights. *Int J Mol Sci*. 2019;20:5615.
[52]. Gan L, Duan H, Xu Q, et al. Human amniotic mesenchymal stromal cell transplantation improves endometrial regeneration in rodent models of intrauterine adhesions. *Cytotherapy*. 2017;19:603-616.